

1 **SUPPORTING INFORMATION:**

2 **Size-Resolved Field Performance of Low-Cost Sensors for Particulate Matter Air**

3 **Pollution**

4 Emilio Molina Rueda,^a Ellison Carter,^b Christian L’Orange,^a Casey Quinn,^a and John Volckens^{a,*}

5 ^a Department of Mechanical Engineering, Colorado State University, Fort Collins, Colorado 80523, United States

6 ^b Department of Civil and Environmental Engineering, Colorado State University, Fort Collins, Colorado 80523, United States

7 *Corresponding author: john.volckens@colostate.edu

8 [Low-cost sensor descriptions and specifications](#)

9 All three sensors utilize light-scattering to estimate aerosol concentrations, including a focused laser diode to
10 illuminate particles that pass through a small sensing zone and a photodiode (placed near the sensing zone but
11 orthogonal to the direction of laser light propagation) to detect the intensity scattered light across a truncated
12 solid angle. Air flow is drawn through each device by a miniature induction fan.

13 The Plantower PMS5003 is described by the manufacturer as a “digital universal particle concentration sensor”

14 ¹. This sensor has been used in multiple commercial low-cost air quality monitors, including the popular
15 PurpleAir (older versions of the PurpleAir used the PMS1003 and newer versions use the PMS6003, but most
16 units including the ones we evaluated use the PMS5003). The Sensirion SPS30 is described by the manufacturer
17 as a particulate matter sensor for air quality monitoring ². Piera describes the IPS-7100 as a “photon counting
18 intelligent particle sensor”, and their technology as “intuitive direct-particle counting” ³. The IPS-7100 firmware
19 is user-upgradable, and we updated from v1.9.9 to v1.9.10 on Piera’s request before the start of our first
20 (fall/winter) data collection period.

21 **Table S1.** Low-cost sensors specifications.

	Plantower PMS5003	Sensirion SPS30	Piera IPS-7100
Stated Outputs			

<i>Mass concentration</i>	PM _{1.0} , PM _{2.5} , PM ₁₀	PM _{1.0} , PM _{2.5} , PM ₄ , PM ₁₀	PM _{0.1} , PM _{0.3} , PM _{0.5} , PM _{1.0} , PM _{2.5} , PM ₅ , PM ₁₀
<i>Number concentration</i>	PC _{0.3} , PC _{0.5} , PC _{1.0} , PC _{2.5} , PC ₅ , PC ₁₀	PC _{0.5} , PC _{1.0} , PC _{2.5} , PC ₄ , PC ₁₀	PC _{0.1} , PC _{0.3} , PC _{0.5} , PC _{1.0} , PC _{2.5} , PC ₅ , PC ₁₀
Cost at quantity of 1	\$15	\$50	\$80
Weight	42 grams	26 grams	26 grams
Size	50 x 38 x 21 mm	41 x 41 x 12 mm	46 x 42 x 12 mm

22

23 We chose these sensors for three reasons: (1) the technology featured in these devices, while similar across the
 24 three models, represents the state-of-the-art for commercial low-cost (<\$100 USD) aerosol sensing; (2) the
 25 selected sensors are from major suppliers that span three continents: Asia (Plantower), North America (Piera),
 26 and Europe (Sensorion); and (3) these sensors (especially the Plantower PMS5003) represent the majority of in-
 27 use technologies across the world. For example, the Plantower has been deployed widely and in large numbers
 28 in networks throughout countries in Asia, like China and Taiwan⁴⁻⁶, where it has a large share of the PM sensor
 29 market. The SPS30 and IPS-7100 were selected because they provide geographic diversity (they are from
 30 companies in North America and Europe, respectively).

31 [Reference monitor operating conditions](#)

32 The EDM 180 is an approved federal equivalent method (FEM) monitor for PM_{2.5} when operated continuously at
 33 a 1.2 L min⁻¹ volumetric flow rate with a Nafion air dryer inside an isothermal inlet^{7,8}. We complied with this
 34 configuration and added the fully temperature-controlled weather protection housing suggested by the
 35 manufacturer. This monitor is also UK-MCERTS certified for PM₁₀⁹.

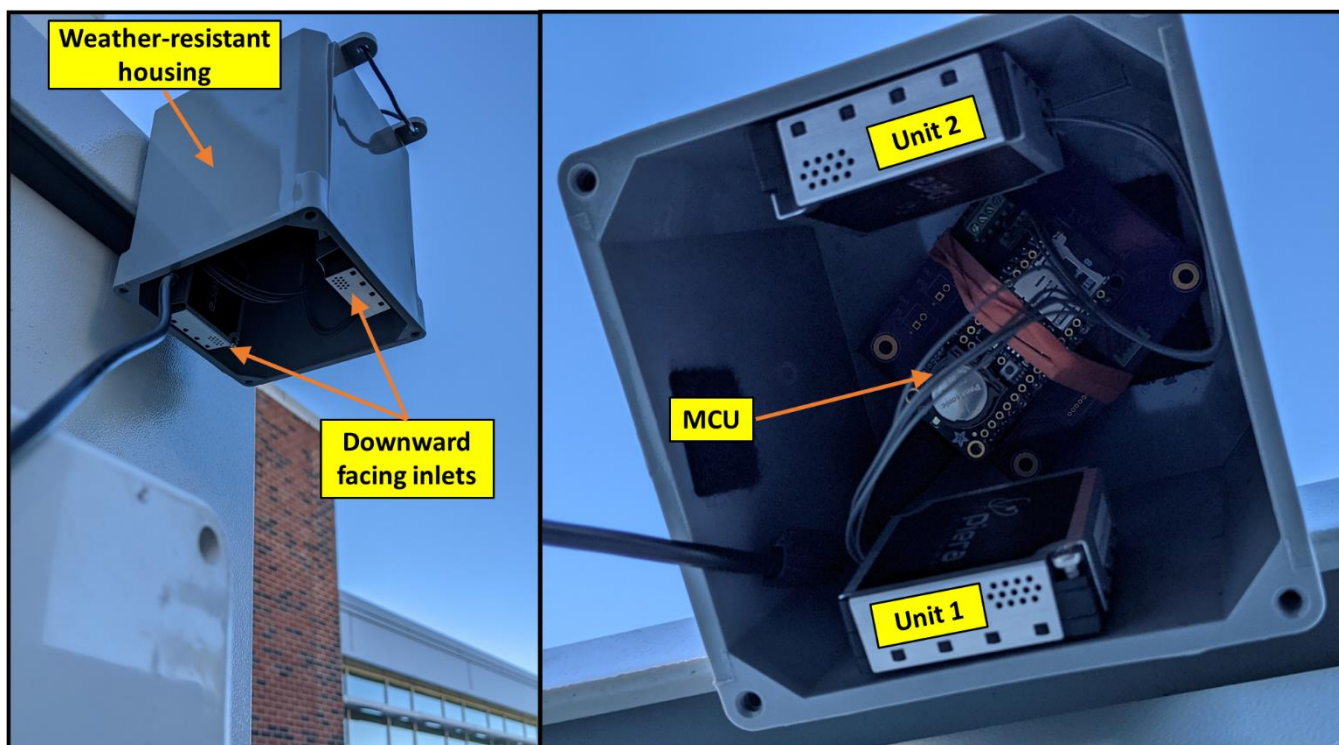
36 [Datalogging](#)

37 We used a PurpleAir PA-II to collect data from two PMS5003 sensors. Logs in CSV format were downloaded from
 38 PurpleAir's website. We developed a custom data logger and housing to collect data from two SPS30 sensors
 39 (Figure S3). The data logger used a Particle Boron LTE microcontroller to read the sensors' data and send it via a

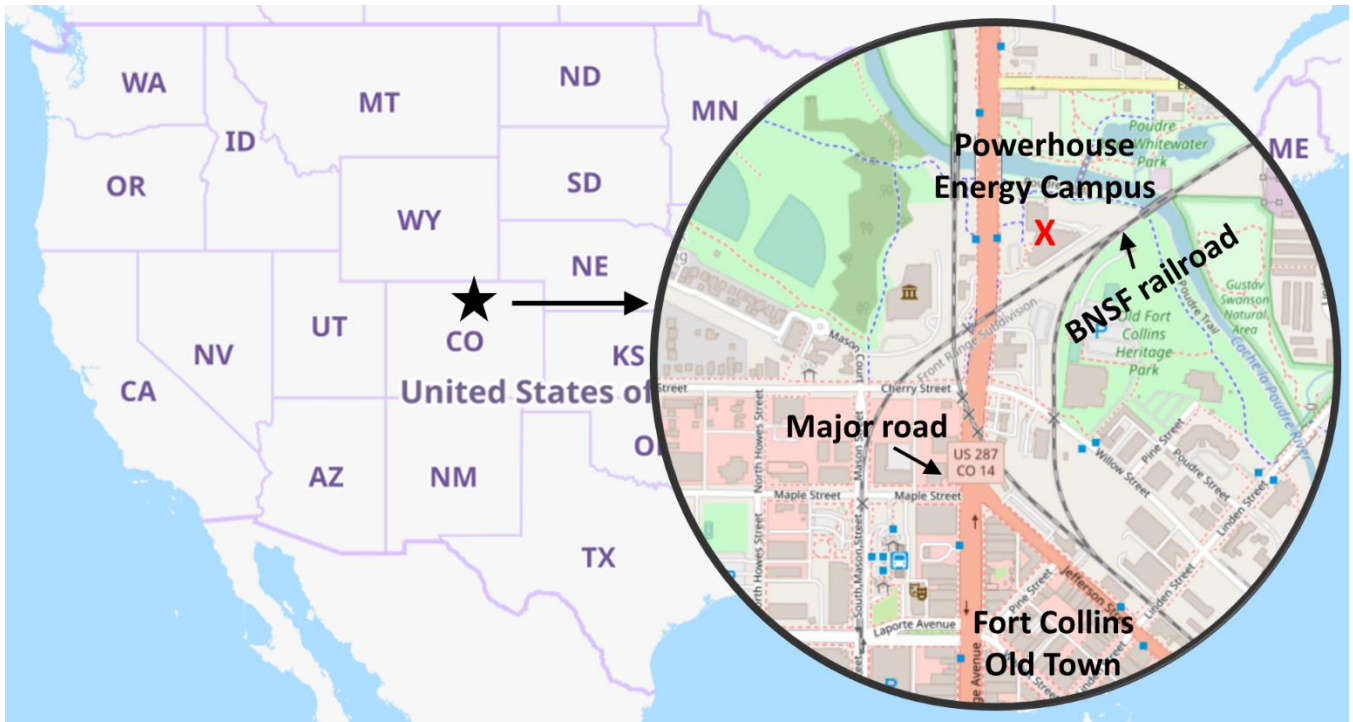
40 cellular network to a server hosted by the Center for Energy Development and Health (CEDH) at Colorado State
41 University. We collected data from two IPS-7100 sensors and sent those data to the server using a Wi-Fi enabled
42 Espressif ESP32 microcontroller. We made a custom housing for the Piera IPS-7100 sensors similar to what we
43 developed for the SPS30 sensors.

44 For the Plantower PMS5003 sensor, the “CF=1, standard particle” output variables were used in all calculations
45 involving PM_{1.0}, PM_{2.5}, and/or PM₁₀ concentrations. The “CF=1” variables from the PMS5003 are uncorrected,
46 according to the manufacturer, as opposed to the “ATM” variables which use a proprietary algorithm and
47 calibration unspecified by the manufacturer to estimate atmospheric aerosol concentrations.

48 One-minute averages of all reported outputs were logged for the SPS30 and IPS-7100 sensors, whereas the
49 PMS5003 (which was operated in a PurpleAir device) logged 2-minute averages. Unless otherwise stated, raw
50 sensor mass and number readings were recorded directly, and only time-based averaging was applied.

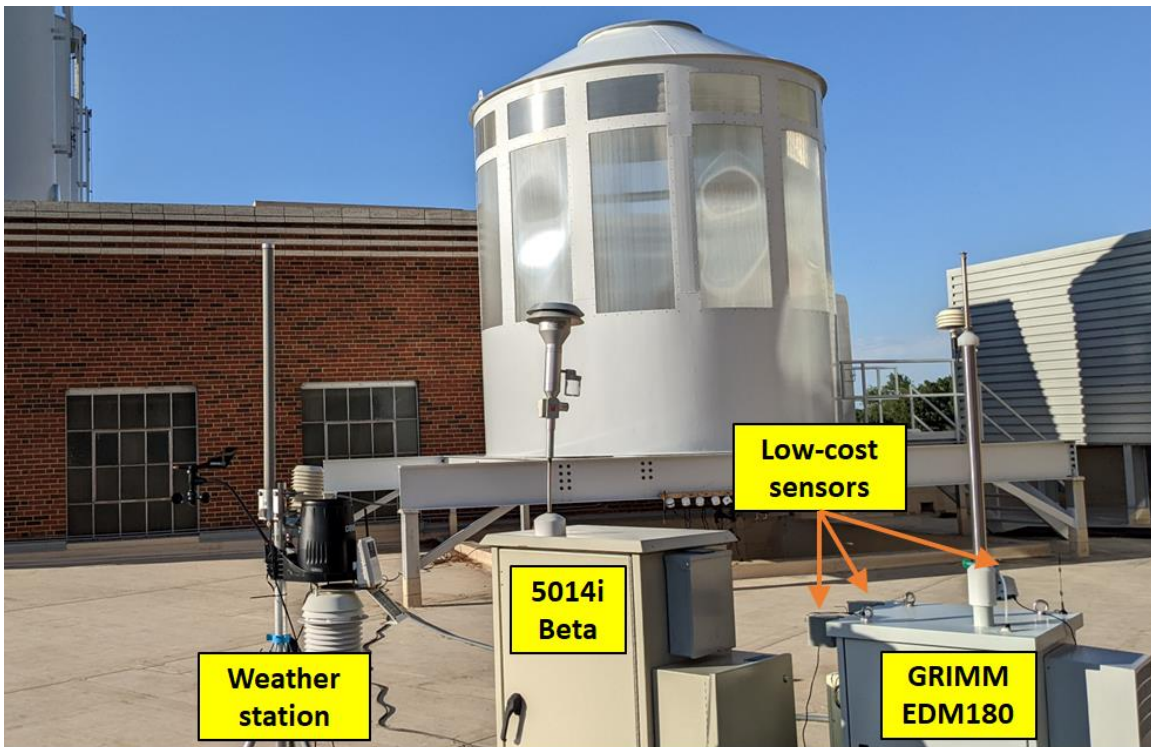


51 **Figure S1.** Data logger and housing used for the IPS-7100 (shown in picture) and SPS30 sensors.
52
53



55
56

Figure S2a. Map of the Powerhouse Energy Campus building in Fort Collins, where the sensors were tested.



57
58
59

Figure S2b. Layout of the instruments used for the field evaluation.

60 Common variables

61 **PM_x**: Cumulative particulate matter concentration up to the particle size indicated by the subscript (in μm).

62 **PM_{a-b}**: Differential particulate matter concentration within the size range indicated by the subscript (in μm).

63 **PM_{a-b}**: Also defined as **PM_b – PM_a**.

64 Statistical analyses

65 Descriptive statistics were calculated for each sensor. We present the statistical metrics corresponding to a
66 single unit (i.e., “unit a”) of each sensor model, except for the metrics that measure intra-model (unit-to-unit)
67 variability. Standard statistical metrics were calculated to assess sensor precision (coefficient of variation among
68 co-located devices of the same model), linearity (coefficient of determination vs. reference), and bias (e.g.,
69 RMSE, MAE, NMB vs. reference) as a function of particle size range. Where appropriate, we developed linear
70 regression models between sensor and reference data using ordinary least squares to estimate slope, intercept,
71 and as inputs to estimate relative expanded uncertainty (REU), which has been adopted by the European
72 Commission air quality directive as a measure of low-cost sensor performance relative to reference monitors¹⁰.
73 Visual diagnostics were used to assess model assumptions (i.e., linearity, normality, and homoscedasticity)
74 (Figures S8 and S9). Time-series and scatter plots were developed to visualize sensor performance as a function
75 of particle size range.

76 Performance metrics - Equations

77 **Root mean square error (RMSE):**

78

$$RMSE = \sqrt{\frac{\sum_{i=1}^n (y_i - x_i)^2}{n}}$$

79 Where n is the number of data pairs, y_i is the i^{th} low-cost sensor measurement, and x_i is the i^{th} reference
80 monitor measurement.

81 **Mean absolute error (MAE):**

82
$$MAE = \frac{1}{n} \sum_{i=1}^n |y_i - x_i|$$

83 Where n is the number of data pairs, y_i is the i^{th} low-cost sensor measurement, and x_i is the i^{th} reference
84 monitor measurement.

85 **Mean bias error (MBE):**

86
$$MBE = \frac{1}{n} \sum_{i=1}^n (y_i - x_i)$$

87 Where n is the number of data pairs, y_i is the i^{th} low-cost sensor measurement, and x_i is the i^{th} reference
88 monitor measurement.

89 **Normalized mean bias (NMB):**

90
$$NMB = \frac{\sum_{i=1}^n (y_i - x_i)}{\sum_{i=1}^n x_i}$$

91 Where n is the number of data pairs, y_i is the i^{th} low-cost sensor measurement, and x_i is the i^{th} reference
92 monitor measurement.

93 **Coefficient of variation (CV):**

94
$$CV = \frac{\sigma}{\mu} = \frac{\sqrt{\frac{\sum (x_j - \mu)^2}{N}}}{\mu}$$

95 Where σ is the standard deviation of the measurements of all units, μ is the mean of the measurements of all
 96 units, N is the number of sensor units, and x_j is the measurement of the j^{th} sensor.

97 **Relative expanded uncertainty (REU):**

98 The European Commission guide to the demonstration of equivalence of ambient air monitoring methods
 99 recommends the following equation to estimate the REU of low-cost sensors ¹⁰:

100
$$REU(y_i) = \frac{2 \sqrt{\frac{RSS}{n-2} - u^2(bs, RM) + u^2(bs, s) + [b_0 + (b_1 - 1)x_i]^2}}{y_i}$$

101 Where n is the number of pairs of collocated data (i.e., reference monitor and LCS), y_i is the low-cost sensor
 102 measurement, and x_i is the reference monitor measurement. The slope and intercept of a linear regression of y_i
 103 as a function of x_i are given by b_1 and b_0 respectively. RSS is the sum of the squared residuals and is calculated
 104 as:

105
$$RSS = \sum_{i=1}^n [y_i - (b_0 + b_1 x_i)]^2$$

106 $u(bs, RM)$ is the between reference method standard uncertainty. Values of this uncertainty are tabulated for
 107 many reference monitors. If not available, it is recommended to use a value of $0.67 \mu\text{g}/\text{m}^3$. This was the case for
 108 our reference monitor.

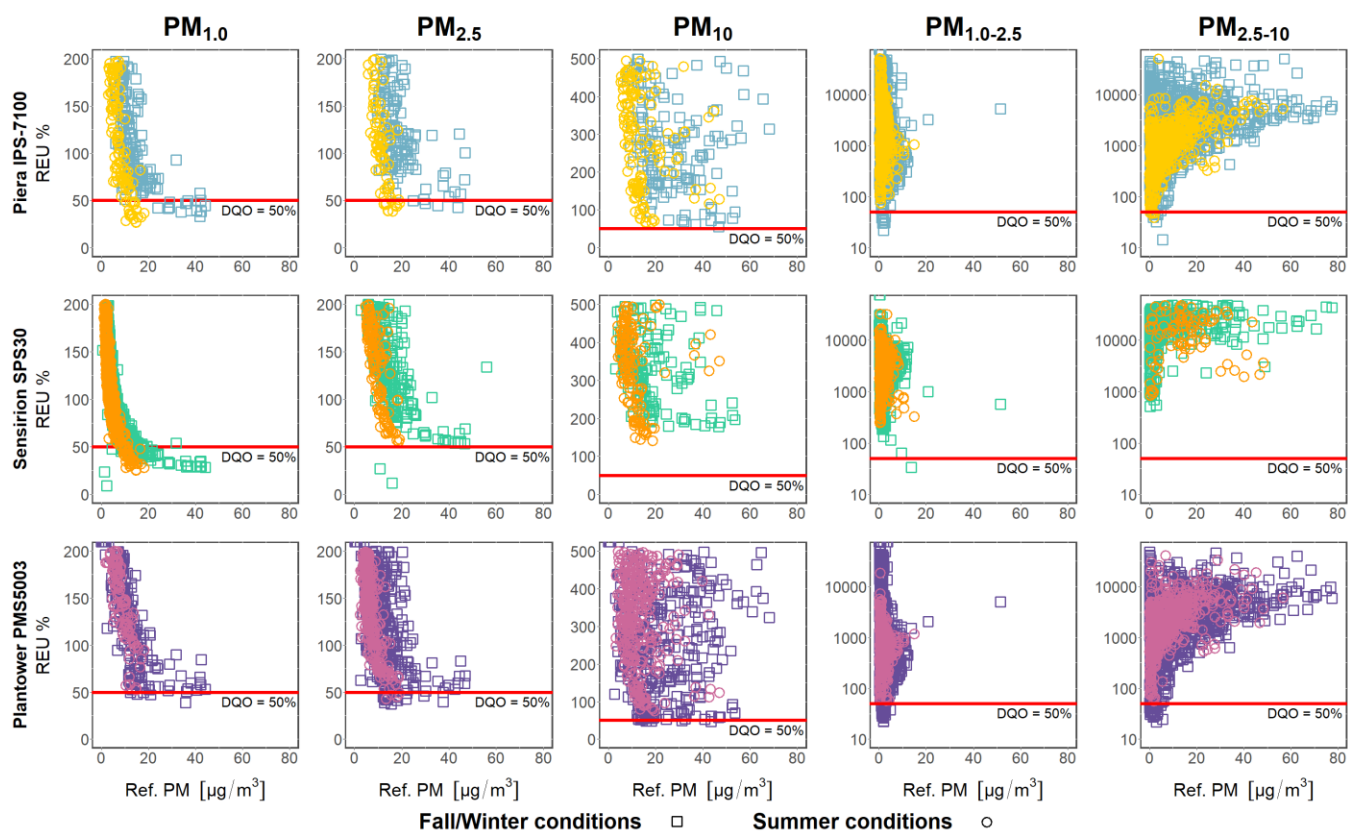
109 $u(bs, s)$ is the between LCS standard uncertainty. When multiple units of the same sensor model are tested,
 110 $u(bs, s)$ can be estimated as:

111
$$u(bs, s) = \sqrt{\left(\frac{\sum_{l=1}^N \sum_{j=1}^p (y_{l,j} - \bar{y}_l)^2}{N(p-1)} \right)}$$

112 Where $y_{l,j}$ is the measurement of sensor unit j for period l . \bar{y}_l is the mean for period l of all sensor units. N is
 113 the number of measurements over time. p is the number of collocated sensor units.

114 Relative expanded uncertainty (REU) plot

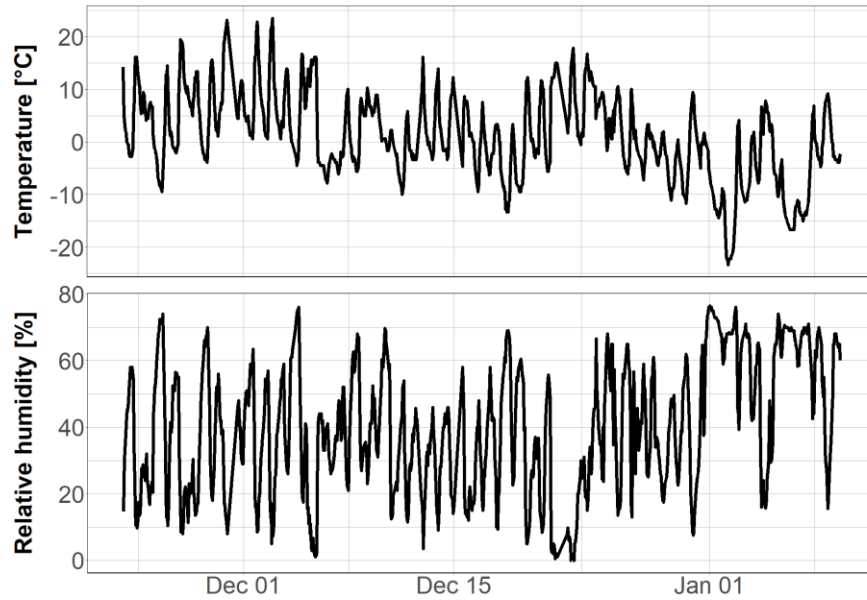
115 The REU plot aids in the qualitative and quantitative analysis of errors. The position of the point on the y-axis is a
116 measure of the bias. The scattering of the points along the y-axis is a measure of noise.



117
118 **Figure S3.** Relative expanded uncertainty (REU) plots for PM estimates from the low-cost sensors. Horizontal axes
119 correspond to the GRIMM EDM180 measurements. The red line is the data quality objective established by the European
120 Commission for low-cost PM sensors (points under the red line have adequate uncertainty). Some points are not shown in
121 the plots due to the axes range.

122 Weather data during the evaluation

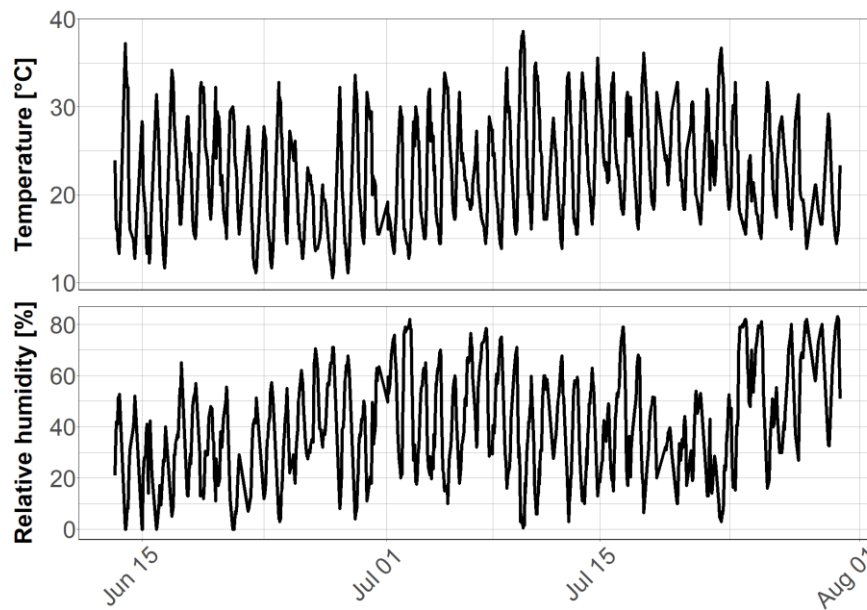
123 The first testing period (23-Nov-2021 to 09-Jan-2022) included late fall and early winter conditions with 13
124 inches of snowfall. Temperature ranged from -22°C to 23°C and relative humidity ranged from 0% to 77%.



125
126

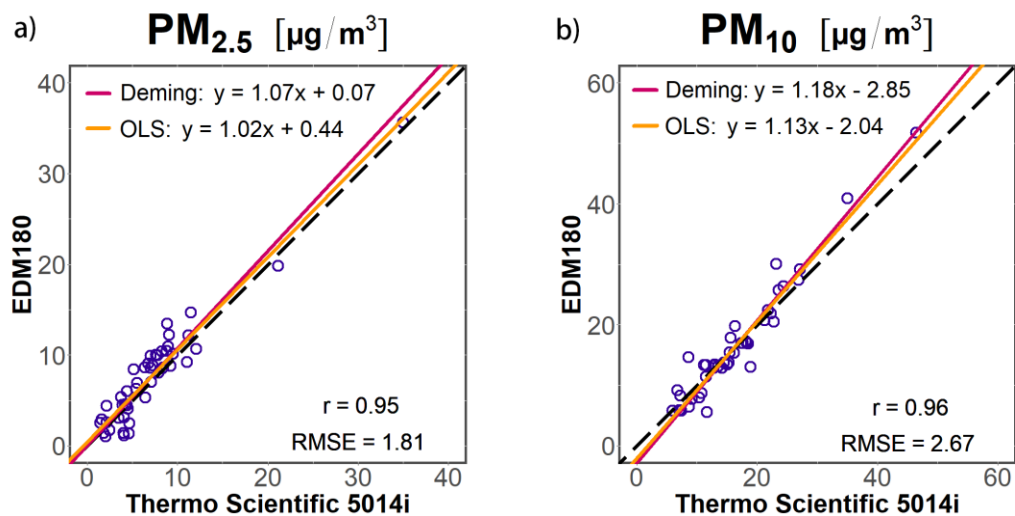
Figure S4. Ambient temperature and relative humidity at 1-hour resolution during the fall/winter campaign.

127 The second testing period (13-Jun-2021 to 30-Jul-2022) was comprised of summer conditions with temperature
128 ranging from 11°C to 38°C and relative humidity ranging from 0% to 82%.



129
130
131

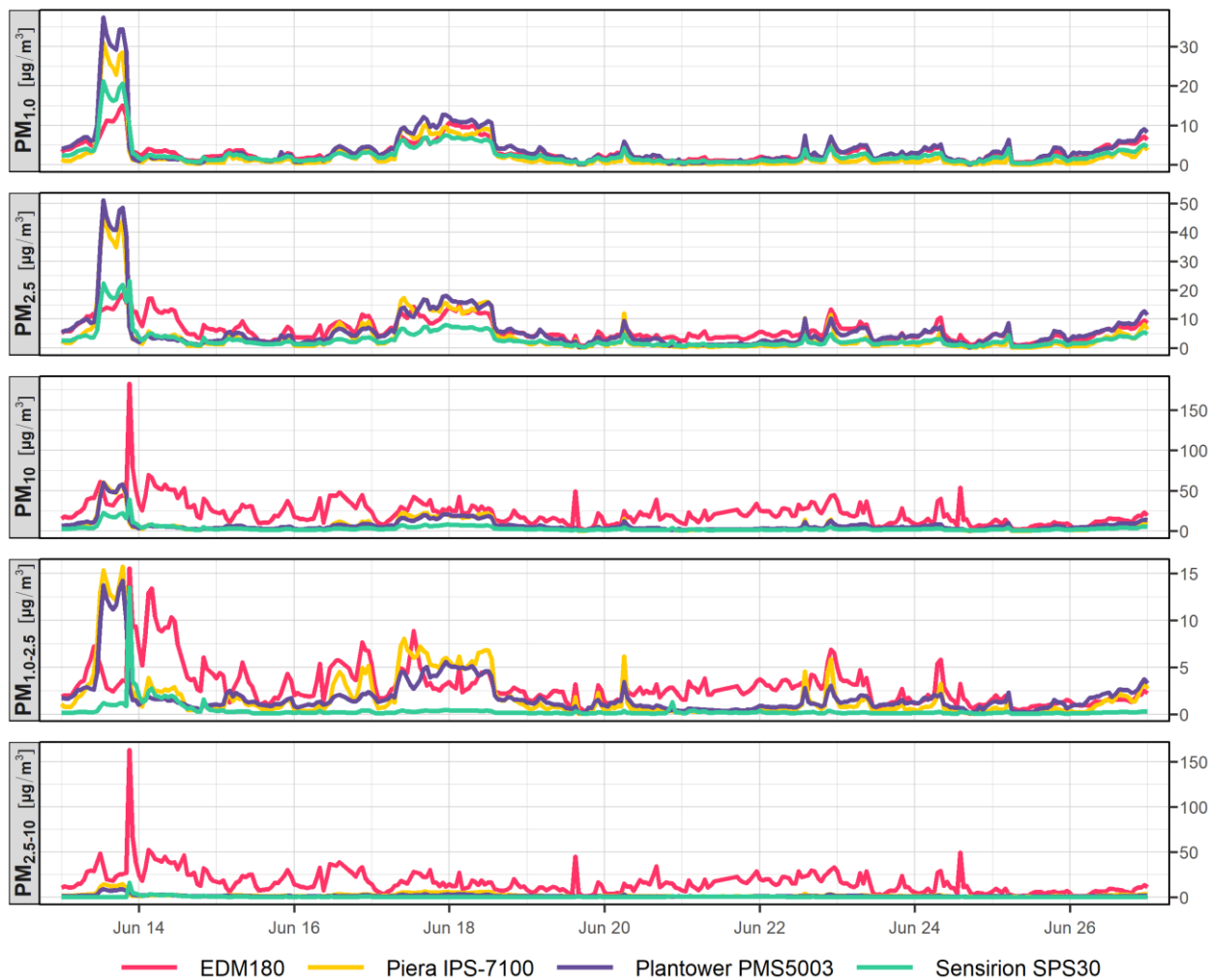
Figure S5. Ambient temperature and relative humidity at 1-hour resolution during the summer campaign.



133

134 **Figure S6.** Scatterplots of PM_{2.5} (left) and PM₁₀ (right) daily concentrations for the GRIMM EDM180 (reference monitor) and
135 the Thermo Scientific 5014i Beta-attenuation monitor (an FEM monitor). The dashed black line corresponds to the “1:1”
136 relationship. Constant error was assumed for the Deming regression.

137 Time-series plot of the summer period



138

139 **Figure S7.** Time series graph of PM concentrations (cumulative and differential) during the first 14 days of the summer
140 period.

141

142

143 Confidence intervals of regression model estimates

144 **Table S2.** Confidence intervals (2.5% to 97.5%) of the model parameters presented on Table 1. The models are linear
 145 regressions of the low-cost sensor vs. the reference monitor (EDM180).

	PM_{1.0}	PM_{2.5}	PM₁₀	PM_{1.0-2.5}	PM_{2.5-10}
Slope					
<i>Piera IPS-7100</i>	0.85 to 0.89	1.64 to 1.76	0.17 to 0.25	0.11 to 0.46	0 to 0.015
<i>Sensirion SPS30</i>	0.86 to 0.89	0.75 to 0.80	0.15 to 0.18	0.19 to 0.26	0.05 to 0.06
<i>Plantower PMS5003</i>	1.41 to 1.46	1.62 to 1.73	0.16 to 0.23	0.07 to 0.23	0 to 0.012
Intercept					
<i>Piera IPS-7100</i>	-1.67 to -1.41	-7.04 to -5.98	1.44 to 3.33	1.04 to 2.09	1.45 to 1.73
<i>Sensirion SPS30</i>	-0.62 to -0.45	-1.60 to -1.18	0.46 to 1.22	-0.26 to -0.05	-0.60 to -0.40
<i>Plantower PMS5003</i>	-1.17 to -0.84	-3.41 to -2.61	5.04 to 6.82	1.95 to 2.44	1.36 to 1.68

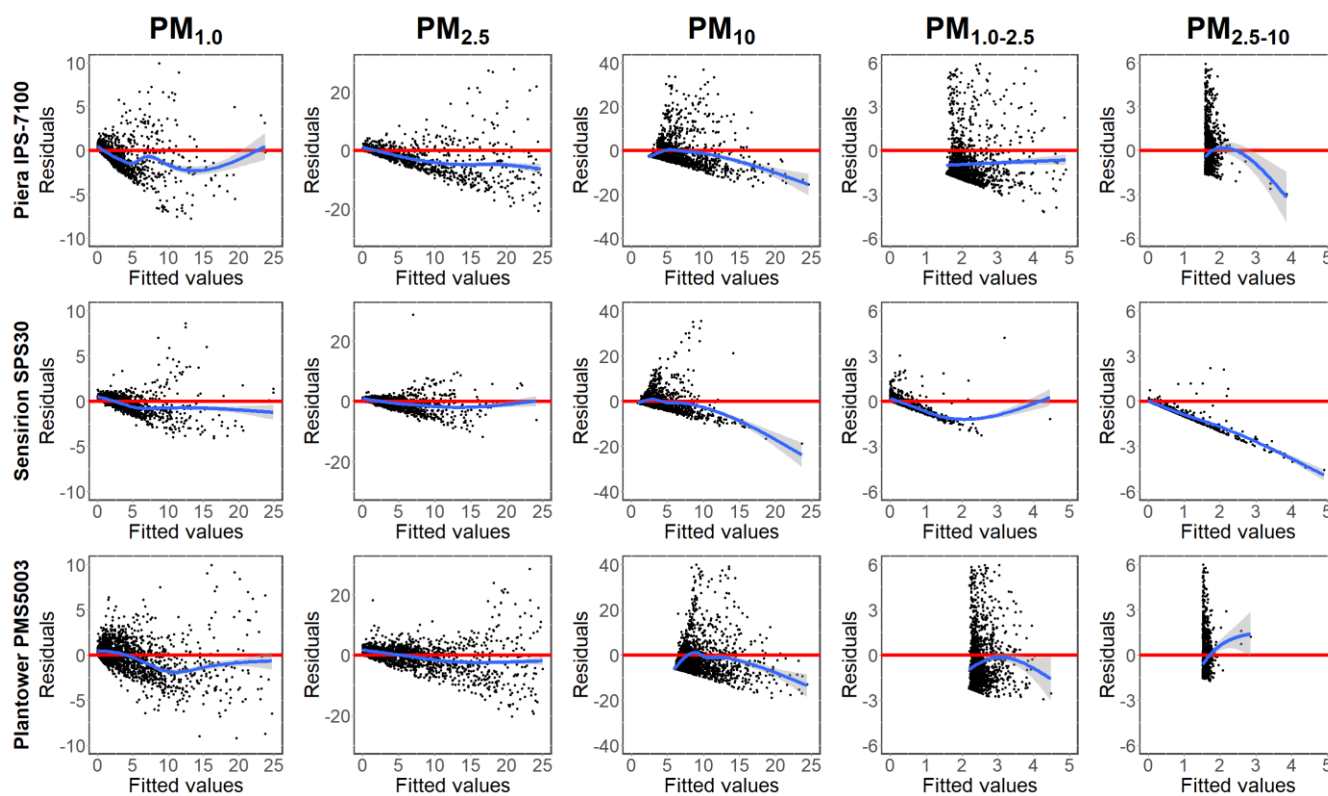
146

147

148 Residual plots of the linear models used in the study

149 Residual plots are mainly used to evaluate the assumptions of a linear model, such as homoscedasticity,
150 independence, and normality. Qualitatively, a “good model” will have residuals that are uncorrelated
151 (independent), normally distributed and centered around the zero line, and constant with respect to the
152 magnitude of the predicted value (homoscedastic). Residuals that do not follow these patterns suggest one or
153 more violations of the assumptions for a linear model (which is often the case for low-cost sensor data and
154 increasingly evident in the larger size fractions).

155



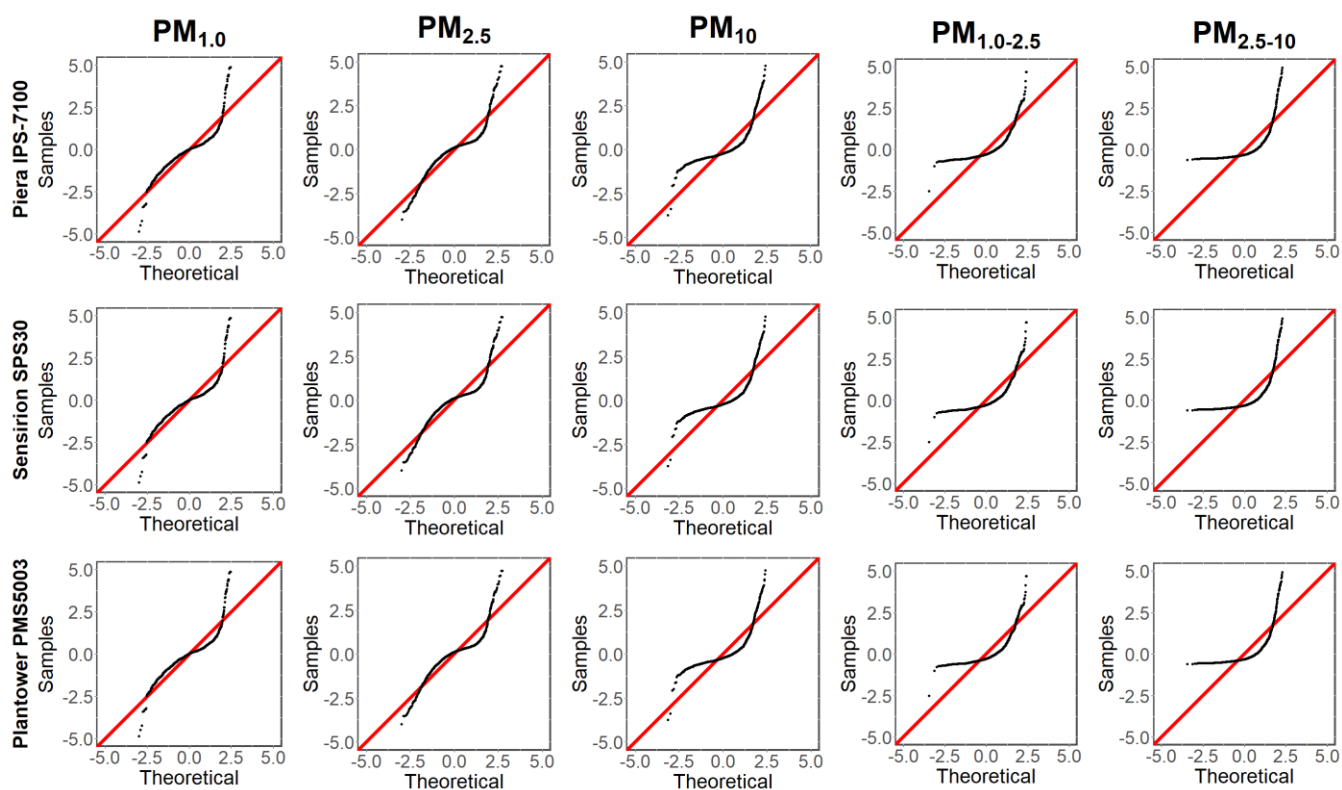
156

157 **Figure S8.** Residual plots corresponding to the low-cost sensor vs. reference monitor linear regression models presented in
158 Figure 2 and mentioned throughout the manuscript. The horizontal red line represents perfect modeled-measured
159 agreement across the range of fitted values; the blue lines represent a LOESS (locally estimated scatterplot smoothing) fit to
160 the observed residuals.

161 [Quantile-Quantile plots of the linear models used in the study](#)

162 Quantile-Quantile plots are used to assess the normality assumption for a linear regression model. The
163 distribution of the residuals (i.e., black dots) is compared against the expected distribution of residuals for an
164 ideal model (i.e., red line). On a “good” Quantile-Quantile plot, the points sit close to the 1:1 line across the data
165 range.

166



167

168 **Figure S9.** Quantile-Quantile plots corresponding to the low-cost sensor vs. reference monitor linear regression models
169 presented in Figure 2 and mentioned throughout the manuscript.

170

171 References

- 172 (1) Yong, Z.; Plantower. *Plantower PMS5003 Data Manual*. [http://www.aqmd.gov/docs/default-source/aaq-](http://www.aqmd.gov/docs/default-source/aaq-spec/resources-page/plantower-pms5003-manual_v2-3.pdf)
173 [spec/resources-page/plantower-pms5003-manual_v2-3.pdf](http://www.aqmd.gov/docs/default-source/aaq-spec/resources-page/plantower-pms5003-manual_v2-3.pdf) (accessed 2022-09-07).
- 174 (2) Sensirion. *Datasheet SPS30*.
175 [https://sensirion.com/media/documents/8600FF88/616542B5/Sensirion_PM_Sensors_Datasheet_SPS30](https://sensirion.com/media/documents/8600FF88/616542B5/Sensirion_PM_Sensors_Datasheet_SPS30.pdf)
176 [.pdf](https://sensirion.com/media/documents/8600FF88/616542B5/Sensirion_PM_Sensors_Datasheet_SPS30.pdf) (accessed 2022-09-07).
- 177 (3) Piera Systems. *Photon Counting Intelligent Particle Sensor for Accurate Air Quality Monitoring Product*
178 *Specification Product Summary*. [https://pierasystems.com/wp-content/uploads/2021/12/IPS-Datasheet-](https://pierasystems.com/wp-content/uploads/2021/12/IPS-Datasheet-V1.1.8.pdf)
179 [V1.1.8.pdf](https://pierasystems.com/wp-content/uploads/2021/12/IPS-Datasheet-V1.1.8.pdf) (accessed 2022-06-29).
- 180 (4) Men, Y.; Li, J.; Liu, X.; Li, Y.; Jiang, K.; Luo, Z.; Xiong, R.; Cheng, H.; Tao, S.; Shen, G. Contributions of
181 Internal Emissions to Peaks and Incremental Indoor PM_{2.5} in Rural Coal Use Households. *Environ. Pollut.*
182 **2021**, 288 (June), 117753. <https://doi.org/10.1016/j.envpol.2021.117753>.
- 183 (5) Li, J.; Men, Y.; Liu, X.; Luo, Z.; Li, Y.; Shen, H.; Chen, Y.; Cheng, H.; Shen, G.; Tao, S. Field-Based Evidence of
184 Changes in Household PM_{2.5} and Exposure during the 2020 National Quarantine in China. *Environ. Res.*
185 *Letts.* **2021**, 16 (9). <https://doi.org/10.1088/1748-9326/ac1014>.
- 186 (6) Cakmak, S.; Dales, R.; Leech, J.; Liu, L. The Influence of Air Pollution on Cardiovascular and Pulmonary
187 Function and Exercise Capacity: Canadian Health Measures Survey (CHMS). *Environ. Res.* **2011**, 111 (8),
188 1309–1312. <https://doi.org/10.1016/j.envres.2011.09.016>.
- 189 (7) Hall, E. S.; States, U.; Protection, E. Reference and Equivalent Methods Used to Measure National
190 Ambient Air Quality Standards (NAAQS) Criteria Air Pollutants - Volume I Authors : Joseph H . Gilliam (
191 EPA / ORD). **2016**, 1 (June). <https://doi.org/10.13140/RG.2.1.2423.2563>.
- 192 (8) United States Environmental Protection Agency. *US-EPA Approval GRIMM EDM180*. [https://www.grimm-](https://www.grimm-aerosol.com/fileadmin/files/grimm-aerosol/Certificates/US-EPA_Approval_GRIMM_EDM180_180_.pdf)
193 [aerosol.com/fileadmin/files/grimm-aerosol/Certificates/US-EPA_Approval_GRIMM_EDM180_180_.pdf](https://www.grimm-aerosol.com/fileadmin/files/grimm-aerosol/Certificates/US-EPA_Approval_GRIMM_EDM180_180_.pdf)
194 (accessed 2022-06-29).
- 195 (9) Sira Certification Service. *PRODUCT CONFORMITY CERTIFICATE GRIMM model EDM 180 / EDM 180+ for*
196 *PM₁₀ and PM_{2.5}*. <https://www.csagroupuk.org/wp-content/uploads/2018/02/MC12019804.pdf>
197 (accessed 2022-06-29).
- 198 (10) European Commission. *Guide to the Demonstration of Equivalence of Ambient Air Monitoring Methods*.
199 [https://www.aces.su.se/reflab/wp-](https://www.aces.su.se/reflab/wp-content/uploads/2016/11/Demonstration_of_Equivalence_of_Ambient_Air_Monitoring.pdf)
200 [content/uploads/2016/11/Demonstration_of_Equivalence_of_Ambient_Air_Monitoring.pdf](https://www.aces.su.se/reflab/wp-content/uploads/2016/11/Demonstration_of_Equivalence_of_Ambient_Air_Monitoring.pdf) (accessed
201 2022-11-02).

202